Dynamics of growth in a three-component mixture with competing interactions

C. Varea
Instituto de Física, Universidad Nacional Autónoma de México, Apartado Postal 20-364, 01000, Distrito Federal, Mexico
(Received 8 April 2003; published 4 June 2004)

We study numerically the dynamics, in two dimensions, of phase separation in ternary mixtures with dipolar interactions which lead to the formation of modulated phases. We distinguish three different modulated phases: a hexagonal phase of droplets, a lamellar phase, and a hexagonal phase of bubbles. Inside the crystal structures an additional phase separation occurs "coloring" the texture. The dynamics in the droplet phase mixes the two kinds of droplets of different composition. The lamellar phase does not evolve toward parallel lamellae, and the phase separation inside the channels proceeds until they reach a grain boundary. The hexagonal bubble phase is never formed due to the phase separation that forms an interface of bubbles which blocks the contact between the two phases. In its place we find an unsuspected lamellar phase.

DOI: 10.1103/PhysRevE.69.061504 PACS number(s): 64.75.+g, 05.45.−a, 64.60.Cn, 68.18.Jk

I. INTRODUCTION

There has been an intense research activity in the problems that arise when studying systems subjected to a rapid quench [1]. Interest has been focused on problems that involve only one order parameter. When the order parameter is scalar we can distinguish two types of systems: simple fluids and fluids with competing interactions. In simple fluids, an initially homogeneous binary mixture that is quenched into a two-phase region phase separates starting to form droplets of the minority phase, which grow in size and number until the volume fraction occupied by the droplets attains its equilibrium value. In the late stages of the separation the larger droplets grow at the expense of the smaller ones. This Ostwald ripening follows a universal growth law driven by surface tension. Lifshitz and Slyozov [2] have developed the phenomenology of this growth in which the average domain size R scales with time t as $R=At^{1/3}$; this has been confirmed experimentally in two-dimensional systems [3,4]. Even when the system is more complex and contains three components, with the possibility of three-phase equilibrium, droplets of two different phases grow, when quenched from a uniform phase, which at late times follow the Lifshitz-Slyozov growth law [5].

When in addition to the surface tension, due to short-ranged attractive interactions, there are also long-ranged repulsive interactions present (as is the case of Langmuir monolayers of polar molecules), undulating phases become stabilized [6]. The problem has been approached from two different view points. McConnell [7] studied single isolated domains and has developed an effective interface free energy for molecular films in the water-air interface where the long-ranged repulsive interactions are dipolar interactions among the single amphiphilic molecules. This free energy contains surface and electric terms which in the case of an isolated circular domain of radius R has the form

$$F = 2\pi R\upsilon^2\left(\ln\frac{e^2\delta}{4R} + \lambda\right), \tag{1}$$

where υ is the dipole density in the monolayer, λ is the line tension, and δ is a short distance cutoff length. Equation (1) has a minimum when $R_{eq}=(e^3\delta/4)[e^{\lambda/\vartheta^2}]$ so that, in this case, domain coarsening is suppressed by the dipolar repulsion. From a different point of view, Andelman [6] and Sagui and Desai [8] have analyzed a free-energy density with short-ranged attractive interactions and long-ranged nonlocal repulsive interactions. Solving the Euler-Lagrange equations in restricted symmetries (lamellar and hexagonal) they obtained a phase diagram which contains five different phases: a uniform gas phase, a droplet hexagonal phase, a lamellar phase, a bubble hexagonal phase, and a dense liquid uniform phase at different concentrations of polar molecules. Sagui and Desai studied the time evolution of these systems through Langevin simulations when the system is quenched, into the droplet phase, and found that after an initial shape transition into the hexagonal phase the system forms modulated patterns broken up by topological defects which anneal away as the system orders. In near critical quenches and in a closely related system, Boyer and Viñals [9] have shown that transient lamellar configurations do not achieve long-ranged orientational order but rather evolve into glassy configurations with very slow dynamics. Here we present the results for the time evolution of a model whose free energy contains two coupled order parameters with long-ranged interaction terms that involve only one order parameter. The result is a competition between modulation and phase separation due to excess free energy at interfaces with line tension that is not compensated by long-ranged repulsive interactions, and the formation of new glassy metastable states that prevent the system from achieving equilibrium. There are several regions of interest in the phase diagram of the model and we present a full account of its dynamical properties as we keep the temperature of the quench constant and vary the concentration in the initial state. In Sec. I we present the model, its phase diagram, and the linear analysis to find the regions of instability. In Sec. II we present our numerical results for the time evolution of the model in several regions of the phase diagram and in Sec. III we present our concluding remarks.

II. THE MODEL

Our model is a three-component lattice model with both short-ranged and long-ranged interactions in the mean-field

approximation. Let u_i^α be the occupation number of species α at site i, then the free energy F is:

$$F = \sum_{i,\alpha} kTu_i^\alpha \ln u_i^\alpha + \frac{1}{2}\sum_{i,j;\alpha,\beta} V^{\alpha,\beta}(r_{i,j})u_i^\alpha u_j^\beta, \tag{2}$$

where T is the temperature and $V^{\alpha,\beta}(r_{i,j})$ is the interaction potential. We consider a fully occupied lattice so that $\Sigma_{\alpha=1}^3 u_i^\alpha = 1$. The interaction potential is attractive for nearest-neighbor sites, zero for second nearest-neighbor sites, and repulsive for third nearest-neighbor ones, with $V^{\alpha,\beta}(r_{i,j}) \sim \nu^\alpha \nu^\beta / r_{i,j}^3$ which corresponds to dipolar interactions with dipolar moment ν^α for species α. Since the lattice is fully occupied there are three independent interaction parameters for the short-ranged interactions, and we use the notation in Ref. [10] for them. For a square lattice this interaction term is

$$\frac{1}{4}\sum_{i,j} au_i^2 u_j^3 + bu_i^3 u_j^1 + cu_i^1 u_j^2$$

where the sum over j is over the four first neighbors of i. We also assume $a+b+c=1$ which sets the temperature and dipolar moments scale. In addition, we use $b=a$, $\nu^1=\nu^2$, and $\nu^3=0$ so that the mixture is symmetric. This leaves us with three dimensionless parameters: the temperature kT, the interaction parameter c, and the dipolar moment ν. In this work we choose $c=0.285$, $kT=0.08$, and $\nu=0.2$. At this temperature the mixture shows, when $\nu=0$, a triple point for a wide range of concentrations in the composition triangle [5]. With $\nu \neq 0$ this grand potential describes a Langmuir monolayer with two different segregating polar molecules in the air-water interface.

The Euler-Lagrange equations, $\delta F/\delta u_i^\alpha = \mu^\alpha$, for the two independent occupation numbers u_i^1 and u_i^2 may be cast in the mean-field form

$$u_i^\alpha = \frac{e^{-(v_i^\alpha - \mu^\alpha)/kT}}{1 + \sum_{\beta=1}^{2} e^{-(v_i^\beta - \mu^\beta)/kT}}, \tag{3}$$

where v_i^α is the functional derivative of the interaction term in F that is calculated by means of Fourier transforms and μ^α is the chemical potential for species α. The Euler-Lagrange equations were solved by successive iterations with a global error $\leqslant 10^{-8}$ and $\mu^1=\mu^2$ (where we expect multiple phase equilibria) starting with different initial configurations with uniform, lamellar, and hexagonal symmetries in a lattice of size 100^2. We also find it convenient to minimize the grand potential $\Omega = F - \Sigma_i \mu^1 u_i^1 - \mu^2 u_i^2$ subject to constant global composition N^α and use

$$N^\alpha = \sum_i u_i^\alpha = e^{\mu^\alpha/kT} \sum_i \frac{e^{-v_i^\alpha/kT}}{1 + \sum_{\beta=1}^{2} e^{-(v_i^\beta - \mu^\beta)/kT}} \tag{4}$$

to adjust the chemical potentials at each step of the iteration in Eq. (3). The model has many minima and with different concentrations and with the same chemical potentials. Calculating the grand potential for each one of them, we find that those with low concentrations of u^1 or u^2 are the most stable ones. We then calculate the grand potential Ω as a function of $\mu^1=\mu^2$ for different symmetries and locate the first-order phase transitions between phases of unlike symmetries. In Fig. 1 the resulting phase diagram is shown. At small concentrations of polar molecules, at the top of the concentration triangle, we find only uniform states. As we increase the chemical potentials of species 1 and 2 we find a first-order phase transition where the stable state has hexagonal symmetry with droplets rich in polar molecules with $u_i^1 = u_i^2$. The region of immiscibility in the composition triangle generated by this first-order transition is marked by the letter a in the figure. As we continue increasing μ^1 and μ^2 we find a point (point b in the figure) where there is a second-order phase transition. The order parameter for this transition is $u_i^1 - u_i^2$ and the composition of the droplets in these hexagonal phases is rich in either the first or the second component of the mixture. Increasing μ^1 and μ^2 we enter into the region marked by I in the figure. There we have hexagonal phases of *colored* droplets. Since the background regions for both types of droplets are the same, there is no excess free energy for mixing the two types of droplets, and region I is a continuous region where the number of droplets of different types depend on concentration. On the right and the left sides of this region we find only droplets of one *color* which are in equilibrium with each other. At larger values of μ^1 and μ^2 we find a first-order phase transition into a region of lamellar phases. The letter c in the figure marks the gap in composition at this first-order transition. This is followed by a region (region II of Fig. 1) where stripes rich in component 1 (2) alternate with stripes rich in component 3; again the stripes can alternate in any order with lamellae rich in component 3

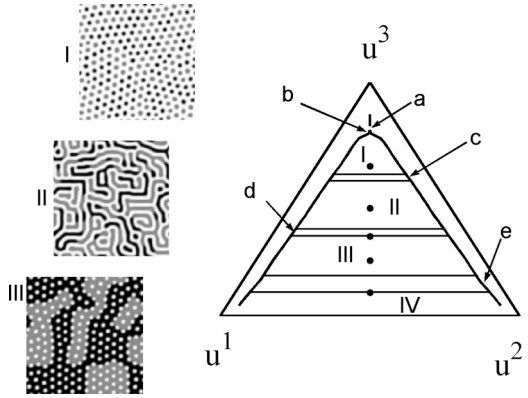

FIG. 1. Phase diagram for the three-component mixture. Italic letters a, c, d, and e mark immiscibility gaps for first-order phase transitions, the point b marks a second-order phase transition where the droplet phases segregate. In region I the stable phases are hexagonal droplet phases with a general appearance shown in inset I. In region II there are lamellar phases as in the inset II. In region III we obtain two-phase equilibria between two hexagonal phases with an interface of bubbles as seen in the inset marked by III. In the insets white regions are rich in component u_3 and black and gray regions are rich in the symmetric components u_1 and u_2. Points represent concentrations $u^1=u^2=0.18$, $u^1=u^2=0.27$, $u^1=u^2=0.33$, $u^1=u^2=0.382$, and $u^1=u^2=0.45$ where we have studied the dynamics.

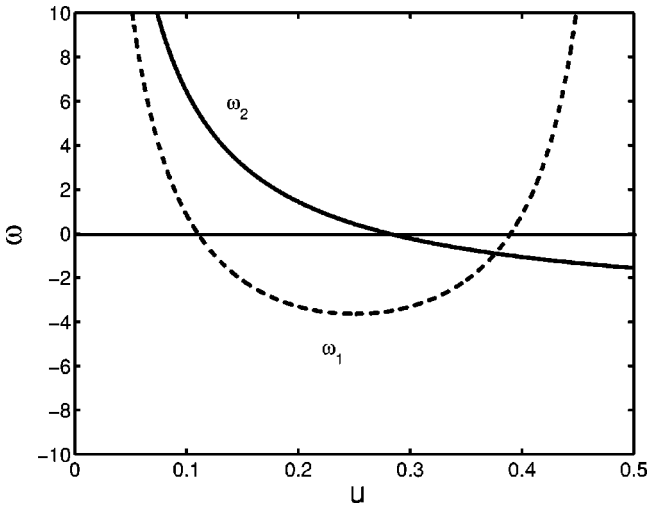

FIG. 2. The two most unstable eigenvalues of the stability matrix as functions of concentration in the symmetric region of the phase diagram.

always between lamellae of component 1 or 2. As in the previous case the states at the right and the left sides of region II are lamellar phases of component 1 in 3 or component 2 in 3, which due to symmetry are in equilibrium. At a larger value of $\mu^1=\mu^2$ we find a first-order phase transition into a region of hexagonal phases, with an immiscible gap marked by the letter *d*. At the right and the left sides of region III of Fig. 1, there is equilibrium between two bubble hexagonal phases. In one of them the background liquid is rich in component 1 while in the other the bubbles reside in a sea rich in component 2. To see the nature of the interface formed when we put these two phases in contact, we solved Eq. (3) with condition (4). The complex interface made of bubbles is shown in the inset III of Fig. 1. Note that the form of the interface is not circular or straight suggesting that there is no excess free energy associated with it. Finally, region *e* of the diagram is the immiscibility gap that leads to region IV where we find two-phase equilibria between two uniform phases; one rich in component 1 and the other rich in component 2 at the right and the left sides of region IV.

It is interesting to analyze the behavior of the stability matrix near uniform states with $u_i^1=u_i^2=u$; its eigenvalues for a lattice vector $\mathbf{k}$ are of the form

$$\omega_1=\frac{kT}{u}+\frac{kT}{1-2u}+V^{1,1}(\mathbf{k})+V^{1,2}(\mathbf{k}) \tag{5}$$

and

$$\omega_2=\frac{kT}{u}+V^{1,1}(\mathbf{k})-V^{1,2}(\mathbf{k}). \tag{6}$$

ω_1 corresponds to fluctuations with $\Delta u^1=\Delta u^2$ and has a minimum at a wave vector $\mathbf{k}_1=(0,1.07)$, and ω_2 corresponds to fluctuations with $\Delta u^1=-\Delta u^2$ with a minimum at a wave vector $\mathbf{k}_2=(0,0)$. In Fig. 2 ω_1 and ω_2 at the values $\mathbf{k}_1$ and $\mathbf{k}_2$ respectively, are plotted as functions of u. There we see that uniform states become unstable to fluctuations with $\Delta u^1=\Delta u^2$ at $\mathbf{k}_1=(0,1.07)$ for values of u in the range $0.11<u<0.38$ and to fluctuations with $\Delta u^1=-\Delta u^2$ at $\mathbf{k}_2=(0,0)$ for $0.28<u<0.5$.

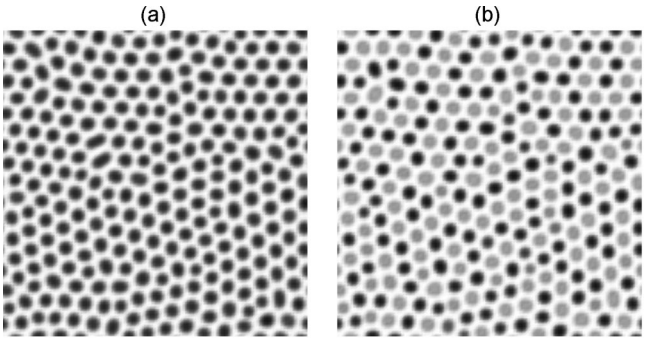

FIG. 3. Evolution of the system for $u_0=0.18$, inside region I, after (a) 75 000 and (b) 150 000 iterations. The tones of gray represent values of the parameter $1-u_i^1-0.5u_i^2$.

The time evolution of the system, after a quench from a uniform phase, is described by the equations

$$\frac{du_i^\alpha}{dt}=\sum_j\frac{\delta\Omega}{\delta u_j^\alpha}-4\frac{\delta\Omega}{\delta u_i^\alpha} \tag{7}$$

for a system with conserved order parameter. In Eq. (7) the sum over j is over the first neighbors of i. Linear analysis shows that fluctuations of the form $\delta u=e^{-\omega t}e^{i\mathbf{k}\cdot\mathbf{r}}$ are solutions of the kinetic equations with $\omega=k^2\omega_i$, where ω_i are the two eigenvalues of the stability matrix in Eqs. (5) and (6).

III. NUMERICAL RESULTS

When studying the dynamics of the system, we used several initial conditions with $u_i^\alpha=u_0+\Delta u_i^\alpha$, where Δu_i^α is a fluctuation with zero mean, the average composition u_0 for components 1 and 2 being the same. The evolution equations were solved by a simple Euler method with a time step $\Delta t=0.006$.

Figure 3 shows typical configurations after 75 000 and 150 000 iterations for $u_0=0.18$, inside region I. Linear analysis shows that the unstable fluctuations are concentration fluctuations with $\Delta u_i^1=\Delta u_i^2$. Following the quench the system forms a complex pattern of interconnected domains. After around 30 000 iterations, the system already shows a short-ranged liquidlike hexagonal structure of dense droplets with $u_i^1=u_i^2$ and $u_i^1+u_i^2=0.9$. At this density, fluctuations with $\Delta u_i^1=-\Delta u_i^2$ become unstable and the droplets start to decompose into droplets rich in component 1 or 2. Since the line tension between the dense droplets and the gas is larger than that of the decomposed droplets with $u_i^1=u_i^2$, these grow in size. In Fig. 4(a) the appearance of the pattern after 1.5×10^6 iterations is shown. We have analyzed the evolution of the underlaying hexagonal structure using Voronoi and triangular representations and followed the evolution of the number of sites, n_z, with coordination z. We find that, very soon, there are only sites with $z=5,6$, and 7. The defects with $z=5$ and 7 pair and evolve very much in the same way as Sagui and Desai [8] have described; through T_1 and T_2 pro-

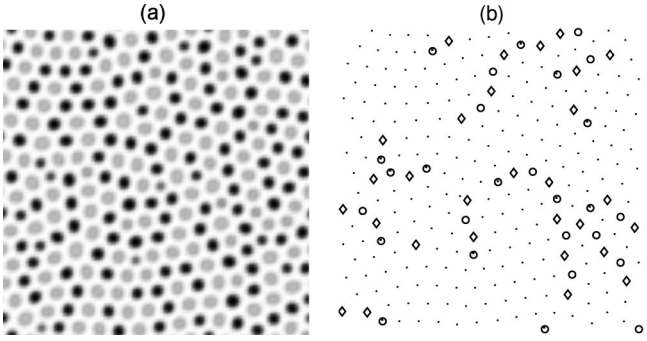

FIG. 4. (a) Appearance of the pattern for $u_0=0.18$ after 1.5×10^6 iterations. (b) A Voronoi construction is shown for the configuration shown in (a). The points marked by a dot have coordination $z=6$, those marked by circles have $z=5$, the circles with a dot inside mark the position of unsegregated droplets, and the diamonds are the positions of droplets surrounded by seven neighbors.

cesses forming boundaries between the different hexagonal grains in this polcrystalline structure. There is however a difference; the average number, $n=(n_5+n_7)/(n_5+n_6+n_7)$, of defects decreases with a growth law that seems to be slower than that found by Sagui and Desai and $n\propto t^{\beta}$ with $\beta\simeq\frac{1}{4}$. We attribute this behavior to the fact that not all the droplets segregate; at very late times we still see droplets with concentrations $u^1=u^2$, and since these are smaller, they tend to pin defects with coordination $z=5$. In Fig. 4(b) this behavior is shown. After 1.5×10^6 the structure is nearly stationary and when we use the state shown in Fig. 4(b) as the initial iteration for the solution of the Euler-Lagrange equation (3), the resulting solution is very close to the initial configuration. There are three causes for the freezing of the liquidlike state: first there are finite size effects where the periodic boundary conditions do not match the wavelength of the structure and impose strain in the lattice, second the quench temperature is very deep, and third the unsegregated droplets pin defects with coordination $z=5$. At early times the system orders both positionally and orientationally and in Fig. 5(a) we can see the measured time evolution (averaged over four runs) of the number of defects and the orientational order parameter $f_6=|\Sigma_k\,\Sigma_\theta\, e^{i6\theta}S_{u^3,u^3}(k,\theta)|$, where $S_{u^3,u^3}(k,\theta)$ is the normalized structure factor of the third component of the mixture. Its evolution is also jammed by finite size effects and the pinning of defects so that the structure is still liquidlike. In Fig. 5(b), clearly the two-step evolution of the system by plotting the behavior of the time evolution of the grand potential is seen; here the first rise in the $\ln(-\Omega)$ curve corresponds to the formation of nonsegregated droplets while the second corresponds to their segregation. There is a purely kinetic effect in the structure that induces an additional correlation; droplets rich in component 1 are surrounded, on average, by four droplets rich in component 2 and two droplets rich in component 1 because growing droplets feed from its neighbors and a growing fluctuation with $u_i^1-u_i^2>0$ induces fluctuations with $u_i^1-u_i^2<0$ in its neighbors. Since there is no interfacial free energy associated with the mixing of the two equilibrium phases of droplets there is no reason for them to unmix; this is shown in Fig. 5(c).

For $u_0=0.27$, inside region II of Fig. 1 (where there are lamellar phases), linear analysis shows again that the unstable fluctuations are of the form $\Delta u_i^1=\Delta u_i^2$. In the dynamics, alternating lamellae of a dense unmixed fluid and a fluid rich in component 3 are very soon formed with a structure that is full of disclinations and dislocations as in Fig. 6(a), after 40 000 iterations. The subsequent evolution, after 80 000 iterations, is a complex mixture of annihilation of defects and the unmixing of components 1 and 2 in the dense lamellae [see Fig. 6(b)]. In this undirected deep quench, the defects in the stripes pattern are pinned [9] and the phase separation continues until the length of the stripes is the same as the channels that the dense fluid makes in this disordered structure. This kinetics is very slow and in Fig. 6(c) we can see the appearance of the pattern after 1.5×10^6 iterations. We have convinced ourselves that this disordered structure is close to a solution of the Euler-Lagrange equations within an error $<10^{-10}$, and thus it is metastable. In Fig. 7(a) the two time evolution of Ω for this case is shown. The appearance of the pattern shown in Fig. 6(c) is very similar to that which Pomeau and Co-workers [11] classified as labyrinths, but its structure factor lacks the long tail toward long wavelengths which characterizes the labyrinthine structures. This is shown in Fig. 7(b).

The unmixing inside the lamellae creates interfaces with a linear tension and no dipolar forces to contrarrest an Ostwald ripening inside them. To study this we have run simulations with initial conditions with random noise whose amplitude is larger along the (1,1) direction than in the perpendicular one $(1,-1)$. Very soon lamellae along the (1,1) direction are formed and the structure has very few defects. Again, after the formation of the parallel lamellae, the dense stripes begin to decompose. We have measured the second moment in the direction (1,1) of the u^1, u^1 structure factor and found that the growth of the length L of the droplets inside the lamellae is consistent with $L\sim t^{1/3}$ as in the Lifshitz-Slyozov universal law but very soon finite size effects become important and we need a larger sample to be sure of this exponent. The final result, shown in Fig. 8, is a lamellar structure with liquids rich in the 1, 2, and 3 components alternating with very few interfaces of liquids rich in components 1 and 2 present. As in the case of region I the kinetics induces an additional ordering; the lamellae alternate in the form $1,3,2,3,1,3,\ldots$.

For $u_0=0.33$ inside region III of Fig. 1 there are two hexagonal bubble phases in equilibrium. The backgrounds of these two bubble phases are liquids, L_1 and L_2, rich in components 1 and 2, respectively. The early time behavior shows growing fluctuations with $\Delta u_i^1=\Delta u_i^2$ so that a hexagonal bubble phase with $u^1=u^2=0.0003$ forms in a sea of a nonsegregated phase with $u^1=u^2=0.4967$. This nonequilibrium structure evolves eliminating defects, but after about 50 000 iterations the unstable dense fluid segregates forming a complex structure. At later stages of the evolution after 2.5×10^5 the underlaying lattice of bubbles is liquidlike hexagonal as shown in Fig. 9(a). In Fig. 9(b) the pair correlation function g_{u^3,u^3} of the third species in the mixture is shown. The two segregated liquids form interfaces with excess line tension so that regions of L_1 and L_2 nucleate in the presence of the bubbles, the hexagonal lattice of bubbles is then displaced to leave space to the nucleating domains, and the result is that the number of defects n decreases until the

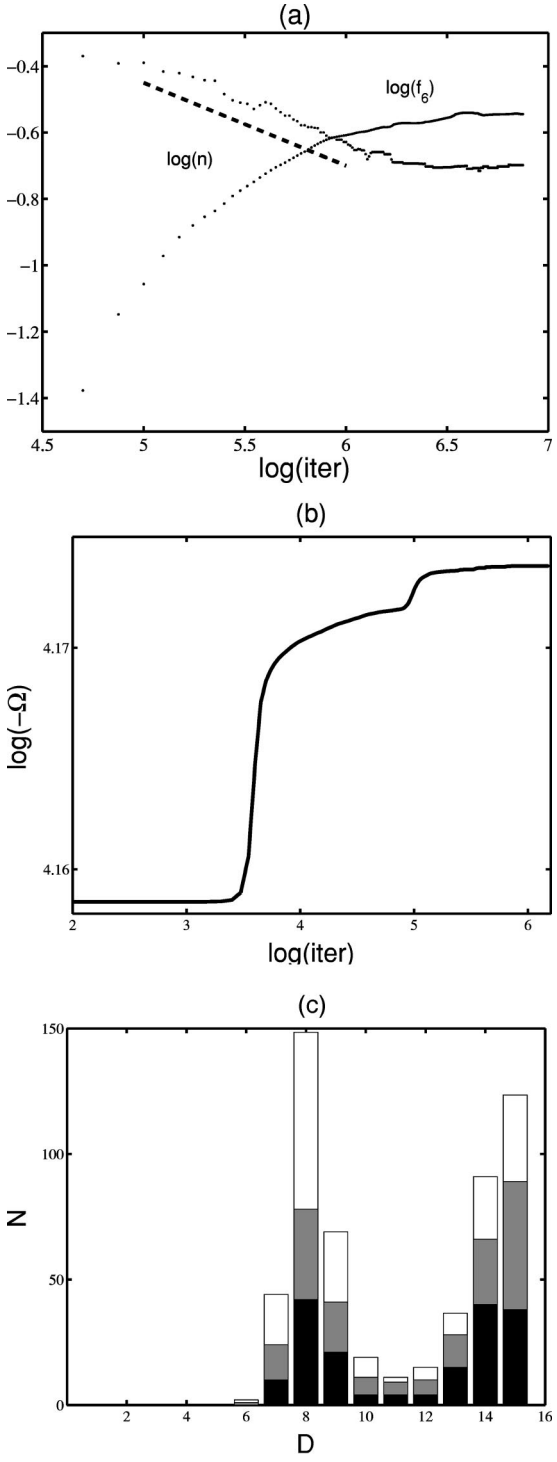

FIG. 5. Properties of the dynamics for $u_0=0.18$. (a) Log_{10}-$\log_{10}$ plot of the normalized number of defects n (dotted line) and the orientational order f_6 (circles; the dashed line is a guide to the eye and has a slope of $1/4$). In (b) Log_{10}-$\log_{10}$ plot of the evolution of the grand potential showing the two time behavior of the model. (c) The distributions of distances is shown. The white portion of the bars is the number of neighbors with unlike *color* while the black and gray portions are the numbers with like *color*.

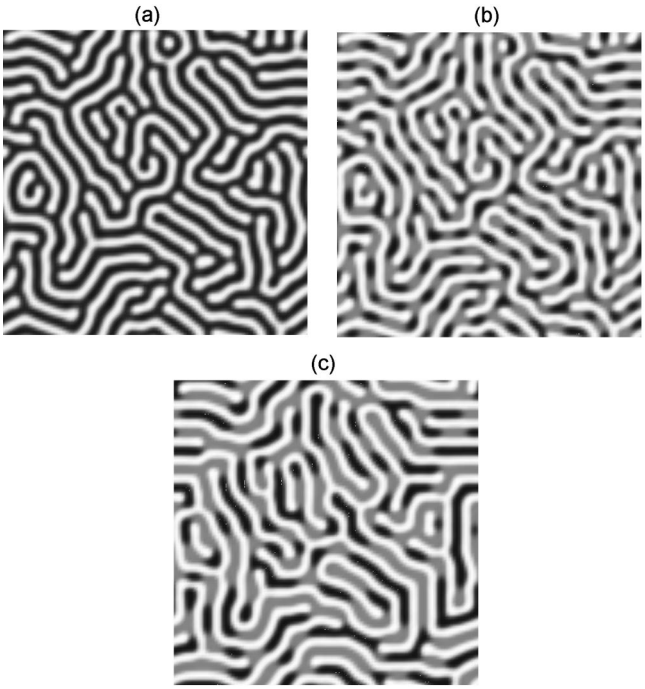

FIG. 6. Evolution of the pattern of lamellae for $u_0=0.27$. (a) After 40 000 iterations the dense regions are in black; (b) after 80 000 iterations where the dense lamellae begin to segregate. (c) The appearance of the pattern after 1.5×10^6 iterations is shown.

liquids start to nucleate and then increases with time as shown in Fig. 9(c).

As we increase the value of u_0 the density of bubbles decreases leaving more space for them to move and for $u_0=0.382$, also inside region III, this motion is more dramatic leading to new lamellar structures. Figure 10 shows typical configurations after 30 000, 60 000, and 1 500 000 iterations. Movies of this evolution have been made and it was observed that as the two liquids segregate they form interfaces with excess line tension. The domains grow in the typical way, with regions of the same liquid coalescing and smaller domains feeding the larger ones; in this process the bubbles are dragged into the interface. Since the dynamics conserves the overall densities of the three components, the number of bubbles remains constant and the segregation continues until the interface is completely saturated by bubbles. We seldom see bubbles leaving the surface and entering the bulk of one of the liquids which is the only way that the equilibrium hexagonal phases could form. Then, the number of bubbles determine the length of the interface and shield the two liquids from each other. In the late time behavior, we see the formation of a new lamellar structure, which has lost completely the original hexagonal symmetry that was present at earlier times, as in Fig. 10(a); the lamellae are of liquids L_1 and L_2 separated by the bubbles in a structure that resembles a two-dimensional microemulsion with the bubbles taking the role of a surfactant. In Fig. 10(c) this late time configuration is shown (after 1.5×10^6 iterations). We have measured the size R of the liquid domains locating the first zero of the angle averaged correlation functions $g_{u^1u^1}$ and $g_{u^2u^2}$; the results are in Fig. 11, there we see, for a decade, a growth

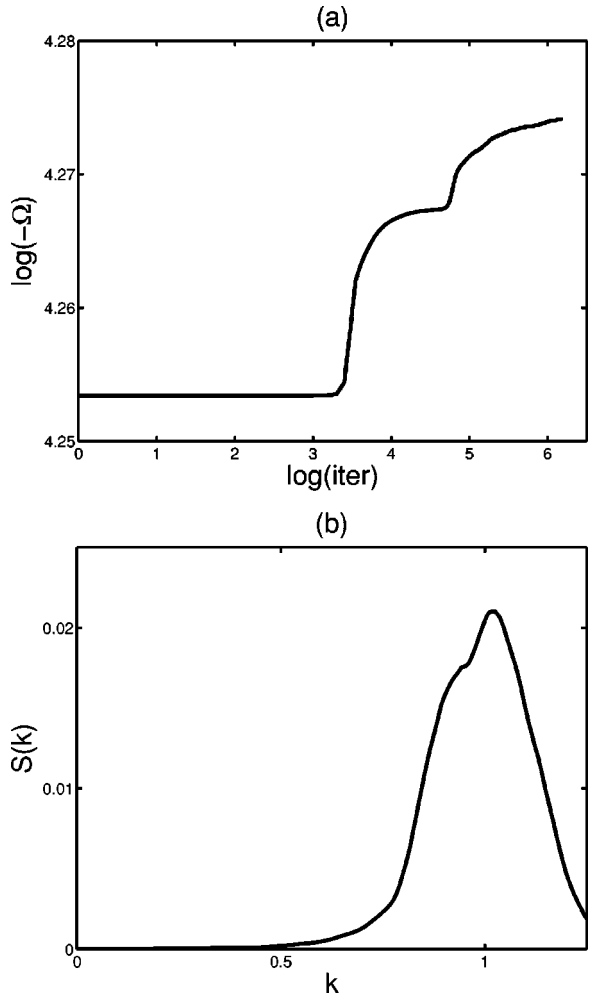

FIG. 7. (a) Log_{10}-$\log_{10}$ evolution of the grand potential showing the two time behavior of the model for $u_0=0.27$. (b) The normalized and angle averaged structure factor of the configuration shown in Fig. 6(c).

law of the form $R\sim t^{1/3}$, where the growth is controlled by line tension, followed by a slowing down once the interfaces between L_1 and L_2 begin to be saturated by bubbles.

It is interesting to confirm that the configuration in Fig. 10(c) is close to a metastable state. As before we have used

FIG. 8. Directed quench for $u_0=0.27$ after 250 000 iterations.

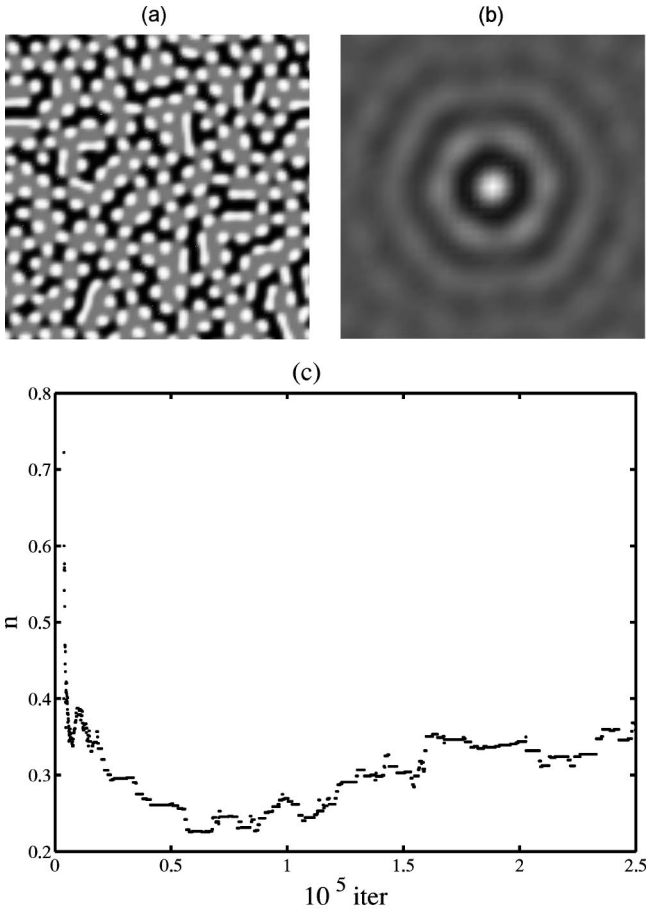

FIG. 9. Some properties of the dynamics for $u_0=0.33$. (a) Appearance of the pattern after 2.5×10^5 iterations. (b) The g_{u^3,u^3} correlation function that shows that the underlaying structure of bubbles has hexagonal symmetry. (c) Evolution of the normalized number of defects n.

this state as the initial configuration in the iteration process of the solution of Eq. (3) with condition (4). The resulting stationary state (with an error $\leqslant10^{-10}$) is indistinguishable from that shown in Fig. 10(c).

As in all regions of the symmetric part of the composition triangle we find that in region III there are many metastable states; the values of Ω for these stationary states are in the range $-2.063\times10^4\leqslant\Omega\leqslant-2.048\times10^4$, the lowest value corresponds to a hexagonal crystal of bubbles, in a single background of L_1 or L_2, while the largest one corresponds to a metastable uniform fluid.

For $u_0=0.45$ in the four-phase region, and close to the L_1-L_2 coexistence region, linear analysis shows that the unstable fluctuations are of the form $\Delta u_i^1=-\Delta u_i^2$ and the two liquids immediately separate. At early times the interface is very long. Since part of component 3 is absorbed in this interface, the bulk phases that condense have less of component 3 than those at the four-phase equilibrium. In Fig. 12 the evolution of the pattern that is forming is shown. As the structure ripens and the interface is reduced, the bulk phases acquire their equilibrium values, and the excess of component 3 goes to the interface where bubbles start to form. It is interesting to see that a bubble at the interface induces the

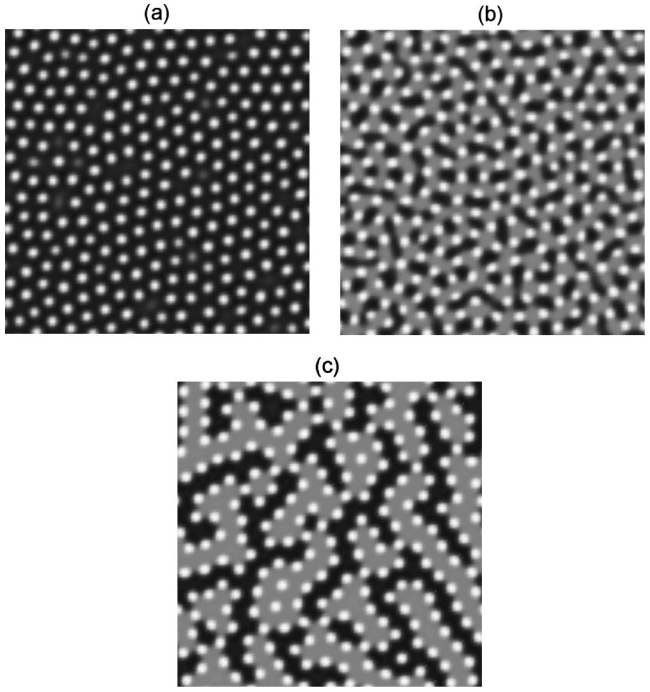

FIG. 10. Evolution of the system for $u_0=0.382$. (a) After 30 000 iterations, (b) after 60 000 time steps, and (c) after 1 500 000 iterations.

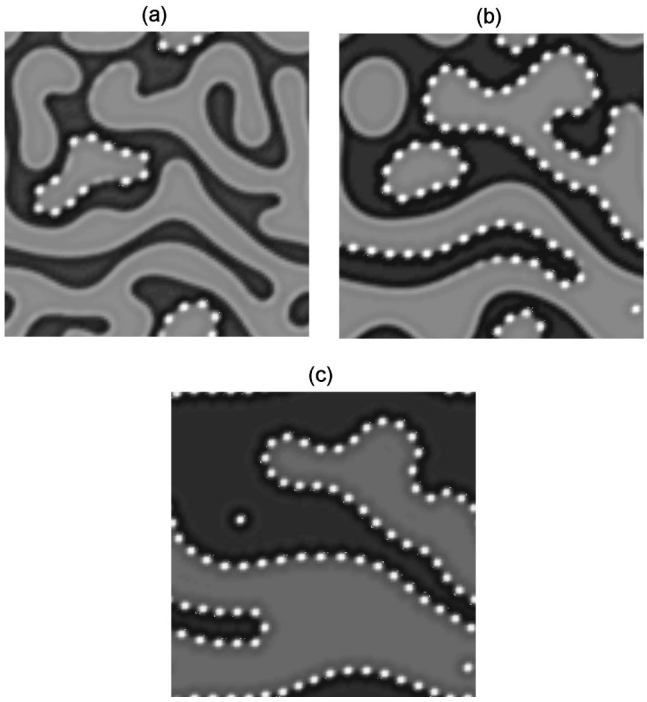

FIG. 12. Evolution of the pattern for $u_0=0.45$. (a) After 210 000 iterations, (b) after 830 000 iterations, and (c) stationary solution of the Euler-Lagrange equations.

formation of neighboring bubbles developing necklaces along the interface. The average size of the domains that were growing at a rate in accord to the Lifshitz-Slyozov law is therefore reduced. The formation of the necklaces is very slow and to have an idea of the final state of the system we have used the configuration shown in Fig. 12(b) into the Euler-Lagrange equations as the initial iteration. The resulting pattern is shown in Fig. 12(c). There we see that the interface has a complex shape, suggesting that there is no cost in free energy for its formation.

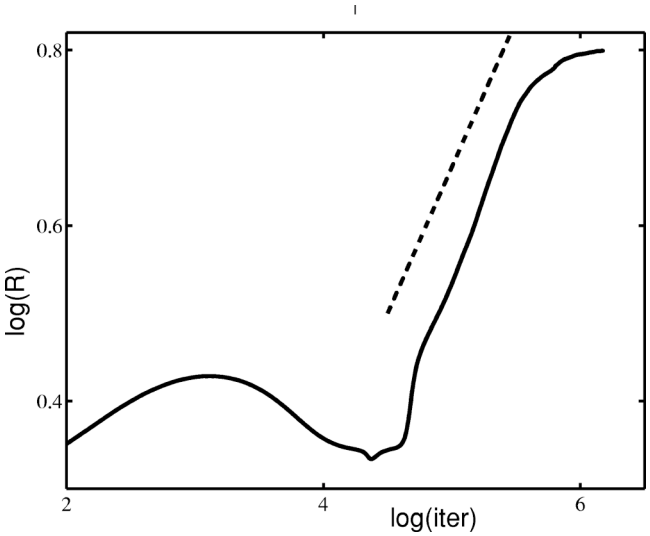

FIG. 11. Evolution of the size R of the liquid domains measured by the first zero of the angle averaged correlation functions $g_{u^1u^1}$ and $g_{u^2u^2}$. In this $\log_{10}$-$\log_{10}$ plot, the dashed line is a guide to the eye and has a slope of $1/3$.

IV. CONCLUSIONS

In summary, we have presented results for the evolution of a model characterized by short-ranged attractive interactions and long-ranged repulsions with two order parameters. We have concentrated on a very symmetric model where the phase diagram has a rich structure with many equilibrium phases. In addition, the model presents innumerable metastable phases and the dynamics often ends up in one of these vitreous states. Moreover, in some regions of the phase diagram, the expected behavior of elimination of defects of the hexagon lattice is disrupted by the segregation of the underlying liquid and the system ends up in new unexpected metastable modulated states where the anticipated hexagonal order is destroyed. We have generalized the model to include two-dimensional Coulomb interactions instead of dipolar interactions. We also have constructed a generalization of the Swift-Hohemberg model free energy with two active order parameters and found the same behavior when the order parameters are conserved, and believe that the properties that we found are those of a wide range of models. I expect that these findings will encourage experiments in mixtures of polar molecules in the water-air interface and related problems.

ACKNOWLEDGMENTS

I acknowledge support from the CONACyT Grant No. 27643-E, and helpful discussions with Denis Boyer.

[1] For reviews, see J. D. Gunton, M. San Miguel, and P. S. Sahni, in *Phase Transitions and Critical Phenomena*, edited by C. Domb and J. L. Lebowitz (Academic Press, New York, 1983), Vol. 3; S. Komura, Phase Transitions **12**, 3 (1998); A. J. Bray, Adv. Phys. **43**, 357 (1994).
[2] I. M. Lifshitz and V. V. Slyozov, J. Phys. Chem. Solids **19**, 35 (1961).
[3] O. Krichevsky and J. Stavans, Phys. Rev. Lett. **70**, 1473 (1993).
[4] M. Seul, N. Y. Morgan, and C. Sire, Phys. Rev. Lett. **73**, 2284 (1994).
[5] C. Varea, Phys. Rev. E **67**, 011508 (2003).
[6] D. Andelman, F. Brochard, and J.-F. Joanny, J. Chem. Phys. **86**, 3673 (1987).
[7] H. M. McConnell, Annu. Rev. Phys. Chem. **42**, 171 (1991).
[8] C. Sagui and R. C. Desai, Phys. Rev. Lett. **71**, 3995 (1993); Phys. Rev. E **49**, 2225 (1994).
[9] D. Boyer and J. Viñals, Phys. Rev. E **64**, 050101 (2001); **65**, 046119 (2002).
[10] D. Furman, S. Dattagupta, and R. B. Griffiths, Phys. Rev. B **15**, 441 (1977).
[11] M. Le Berre, E. Ressayre, A. Tallet, Y. Pomeau, and L. Di Menza, Phys. Rev. E **66**, 026203 (2002).